Available online at www.sciencedirect.com
SCIENCE DIRECT®
Carbohydrate Research 339 (2004) 579–590
Carbohydrate RESEARCH

Inactivated enzymes as probes of the structure of arabinoxylans as observed by atomic force microscopy

Elizabeth L. Adams,[a,†] Paul A. Kroon,[a] Gary Williamson,[a,‡] Harry J. Gilbert[b] and Victor J. Morris[a,*]

[a]*Institute of Food Research, Norwich Research Park, Colney Lane, Norwich NR4 7UA, UK*
[b]*School of Cell and Molecular Biosciences, University of Newcastle upon Tyne, Newcastle upon Tyne NE1 7RU, UK*

Received 23 May 2003; Received in revised form 14 August 2003; accepted 6 November 2003

Abstract—The complex structures of water-soluble wheat arabinoxylans have been mapped along individual molecules, and within populations, using the visualisation of the binding of inactivated enzymes by atomic force microscopy (AFM). It was demonstrated that site-directed mutagenesis (SDM) can be used to produce inactive enzymes as structural probes. For the SDM mutants AFM has been used to compare the binding of different xylanases to arabinoxylans. Xylanase mutant E386A, derived from the Xyn11A enzyme (*Neocallimastrix patriciarium*), was shown to bind randomly along arabinoxylan molecules. The xylanase binding was also monitored following *Aspergillus niger* arabinofuranosidase pre-treatment of samples. It was demonstrated that removal of arabinose side chains significantly altered the binding pattern of the inactivated enzyme. Xylanase mutant E246A, derived from the Xyn10A enzyme (*Cellvibrio japonicus*), was found to show deviations from random binding to the arabinoxylan chains. It is believed that this is due to the effect of a small residual catalytic activity of the enzyme that alters the binding pattern of the probe. Control procedures were developed and assessed to establish that the interactions between the modified xylanases and the arabinoxylans were specific interactions. The experimental data demonstrates the potential for using inactivated enzymes and AFM to probe the structural heterogeneity of individual polysaccharide molecules.

Keywords: Arabinoxylans; Pentosans; Atomic force microscopy; Xylanases

1. Introduction

Arabinoxylans are characteristic cell-wall polysaccharides of noncommeloid monocotyledons that include grasses and cereals.[1–3] An arabinoxylan is considered[4] to consist primarily of a linear backbone of β-(1→4)-linked D-xylose residues that is partially substituted at intervals with individual α-L-arabinose residues attached through O-2 and/or O-3 (Fig. 1). The molecular structure is complex, and the distribution of arabinose side chains along individual molecules, and between molecules in a population, is not known with complete certainty. Present methods of analysis cannot probe the distribution of side chains on individual arabinoxylans. Hence the distribution of side chain residues cannot, at present, be determined with complete certainty, since there are believed to be various patterns even within an arabinoxylan from a single species.[5] The polysaccharides may also contain small amounts of xylose, galactose or glucuronic acid as side chains, in addition to a variety of phenolic residues. Although arabinoxylans are generally considered to be linear molecules, static and dynamic light scattering studies[6] have reported that these polysaccharides may not be simple linear structures, but may exhibit some degree of branching. The chemical structures of arabinoxylans are potentially

* Corresponding author. Tel.: +44-1603-255271; fax: +44-1603-5077-23; e-mail: vic.morris@bbsrc.ac.uk
† Present address: Department of Surgery, Quillen College of Medicine, East Tennessee State University, Johnson City, TN 37614, USA.
‡ Present address: Nestle Research Centre, PO Box 44, Lausanne CH-1000 Lausanne 26, Switzerland.

0008-6215/$ - see front matter © 2003 Elsevier Ltd. All rights reserved.
doi:10.1016/j.carres.2003.11.023

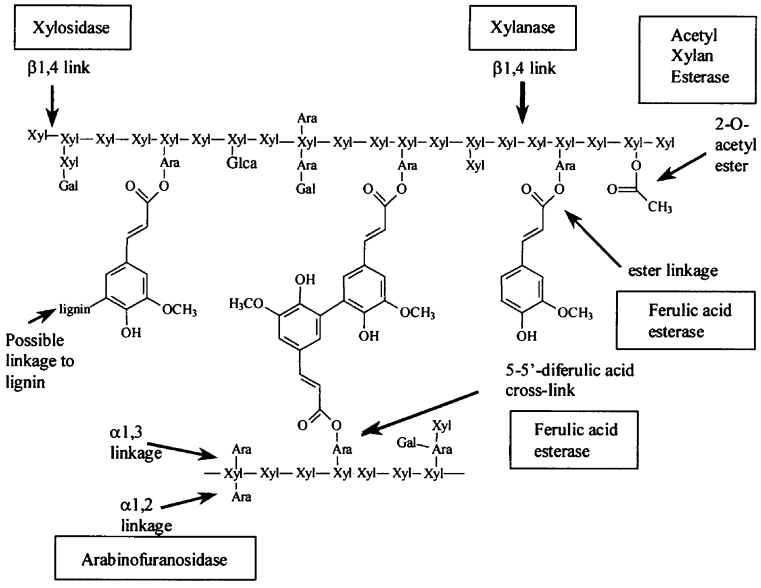

Figure 1. Schematic depiction of the main structural features considered present within water-soluble wheat arabinoxylans. The diagram also indicates the linkages cleaved by a variety of enzymes that are active against arabinoxylans.

heterogeneous both within a given polysaccharide and between polysaccharides. The complexity of the molecular structure will influence the interaction of xylanases with arabinoxylans. Arabinose residues are the main substituents along the xylan backbone and so have the greatest influence on xylanase binding. The presence of unsubstituted or 'smooth' regions (of between two and five, or possibly more xylose residues) are thought to be found between substituted regions that range from highly ordered to completely random arrangement of substitutions.[7–9] The complexity of the interaction means that enzymes like xylanases could provide sensitive probes of the chemical structure. At present, hydrolysing the polysaccharide and then analysing the fragmentation patterns produced exploits this sensitivity to chemical structure. Thus this approach can be used to identify different patterns of side chain substitution that are present within the ensemble of molecules. However, this type of approach cannot distinguish features that are characteristic of all the molecules present from those that are only present in sub-populations of arabinoxylans. More information could be obtained if the binding of the enzyme to the polysaccharide could be visualised. Such an approach would require inactivation of the enzymes.

Xylanases and arabinofuranosidases are important enzymes that are used routinely for industrial treatment of arabinoxylans. Xylanases (EC 3.2.1.8) belong to one of two glycoside hydrolase families (GH10 and 11) and their biological function (the depolymerisation of xylans) is often exploited commercially in the pulp, paper, food and animal feed industries.[10] Arabinofuranosidases are a group of enzymes capable of hydrolysing the arabinofuranosidic linkages[11,12] present in arabinoxylans (Fig. 1). The structure of many xylanases has been elucidated[11–17] and the molecular mechanism of hydrolysis of the xylosidic linkage is understood in quite specific terms.[18,19] The use of X-ray crystallography, protein chemistry, enzymology and site-directed mutagenesis[20] has made it possible to determine the amino acids that play a critical role in substrate binding and catalysis in GH10 and GH11 xylanases. Specific chemicals have been identified for modifying targeted amino acids.[21] *N*-Bromosuccinimide (NBS) oxidises tryptophan residues present in xylanases,[22] and 1-ethyl-3-[3-(dimethyl amino)propyl]carbodiimide (EDCI) modifies carboxylic acid groups present at the active site of many enzymes.[21] These techniques, together with site-directed mutagenesis (SDM), can be applied to produce chemical and genetic mutants that bind but do not hydrolyse arabinoxylans. The possibility of directly studying the interaction of such mutants with arabinoxylans, by imaging these binding events by atomic force microscopy (AFM), provides an important first step towards understanding both the complex heterogeneous chemical structure of arabinoxylans and its effect on enzyme binding.

Previous AFM images of arabinoxylans[23,24] have revealed stiff extended polymeric structures with a calculated Kuhn statistical segment length of 128 nm. The majority of the polymeric structures seen were found to be linear chains, but a small fraction was found to be branched. For all the samples examined the relative number of branched chains was about 15%. Branches appeared to be randomly located on the backbones and the likelihood of a branch occurring on a particular

chain was shown to increase with increasing contour length. The present paper demonstrates how AFM can be used in combination with active and inactive enzymes to further characterise the complex structures of individual arabinoxylan molecules.

2. Results and discussion

As described previously[23] neutral sugar and methylation analysis confirmed that the extracted polysaccharide was a typical water-soluble wheat arabinoxylan containing xylose and arabinose (98%), together with small amounts (2%) of glucose, galactose and mannose. Methylation analysis demonstrated the presence of terminal xylose and (1 → 4)-linked xylose. Equal quantities of xylose residues containing 2,3- and 3-linked arabinose were identified. However, no detectable amounts of purely 2-linked arabinose were found. The level of backbone substitution with arabinose was found to be 0.55.[23] The estimated levels of ferulic acid, di-ferulic acid and protein were 0.89, 0.09 and 1.8 mg g^{-1}, respectively. Only 5–5, 8-O-4′ and 8–5′ ferulic acid dimers were detected in the alkaline extracts.[23]

Xylanase activity was assayed against wheat flour arabinoxylan (Megazyme) and the amounts of reducing sugars released were measured using the DNS assay. The enzyme and polysaccharide were pre-incubated before AFM imaging, which might mean that even low levels of hydrolysis would interfere with the imaging process.

Mutant E386A and mutant E246A from *Neocallimastrix patriciarium* Xyn11A and *Cellvibrio japonicus* (formerly *Pseudomonas fluorescens* subsp. *Cellulose*) Xyn10A, respectively, in which the catalytic nucleophile had been replaced with an alanine, and the catalytic acid/base mutant of Xyn11A (E223A) were analysed for catalytic activity and substrate binding (Table 1). Enzyme activity was assayed (2 h, 30 °C) using wheat flour arabinoxylan (1% w/w in 2 mM ammonium bicarbonate; Megazyme) as the substrate and the reducing sugars released were detected using the DNS reagent. No enzyme activity was detectable for the mutant Xyn11As E223A or E386A (the detection limit using the DNS reagent was 2 mU mg^{-1}). However, the Xyn10A mutant E246A did display detectable activity that was 1000-fold less than the wild-type xylanase. The binding of these enzymes to insoluble wheat arabinoxylan was assessed by spectrofluorimetry (Table 1). Genetic modification of a single amino acid can alter the interactions between amino acids present within the protein and therefore alter the protein. This is illustrated by the differences found in the solubility of the Xyn11A mutants E386A and E233A. The former was found to be soluble across the pH range used in analysis, whereas mutant Xyn11A E223A was only soluble between pH 7 and 9. This illustrates both the importance of the pH of the reaction and the nature of the mutant.

Preliminary AFM measurements on mixtures of arabinoxylans with the Xyn10A mutant E246A also revealed that extended incubation with the enzyme led to some degree of depolymerisation, which was attributed to the low but detectable activity of the mutant enzyme.

If enzyme binding is to be used to probe the polysaccharide structure it is necessary to develop methodologies that minimise or eliminate nonspecific binding of enzymes to the polysaccharides. To provide further evidence that any binding events observed by AFM were the result of specific interactions between xylanases and arabinoxylans control methods were developed. Test samples (xylanase and arabinoxylans) were incubated (overnight, 30 °C) and compared with control samples of xylanase–xanthan and arabinoxylan–polygalacturonase for which there should be no enzyme activity or specific binding. No detected increase in reducing sugars using the DNS assay was observed following the incubation of xylanase from *C. japonicus* with xanthan or after incubation of polygalacturonase from *Aspergillus niger* with arabinoxylans.

The contribution of nonspecific binding in the binding assays used for the modified enzymes can be assessed using the control samples. Possible levels of nonspecific binding were investigated for polygalacturonase and water-insoluble arabinoxylan mixtures by

Table 1. Characterisation of genetically modified xylanases

Property	pH	Control	Mutant Xyn10A E246A	Mutant Xyn11A E386A	Mutant Xyn11A E223A
Activity (μmol min^{-1} mg^{-1})		450	ND	ND	ND
Binding (%)	3	100	95	69	NP
Binding (%)	5	100	94	98	NP
Binding (%)	7	100	92	100	85
Binding (%)	9	100	93	95	65
p*I*		4.0	4.0	4.0	4.0

The control is the active *C. japonicus* Xyn10A xylanase. ND—not detected. NP—not performed due to problems with solubility of the enzyme. Binding values are quoted as % values relative to the control.

spectrofluorimetry. At pH 7 the level of nonspecific binding detected was $\leqslant 2.2\%$ of the total protein added. The level of nonspecific binding was also analysed by AFM imaging of test samples and controls. The negative controls were xylanase from *C. japonicus* imaged together with the polysaccharide xanthan, and polygalacturonase from *A. niger* imaged with arabinoxylans. The positive control imaged under identical conditions was an active xylanase from *C. japonicus* imaged with arabinoxylans. In the case of the positive control it was found that the xylanase can completely hydrolyse the polysaccharide, and no polysaccharide or oligosaccharide fragments were observed by AFM. This indicates that, under the conditions used to investigate modified xylanase binding to arabinoxylans, the native xylanase remains active and hence can bind effectively to the arabinoxylan chains. This confirms that the experimental conditions are such that the AFM should be able to detect specific binding of modified enzymes to arabinoxylans.

The imaging of mutant xylanase binding events along arabinoxylan polymers is an important step in the analysis of xylanase binding and arabinoxylan structural analysis. The possibility of nonspecific binding was assessed by analysis of the AFM images obtained for the test samples (xylanase–arabinoxylans mixtures) and the control samples (xanthan–xylanase and polygalacturonase–arabinoxylan). For the xanthan–xylanase system this was achieved by determining the number of xylanase molecules found to be associated with xanthan polymers when imaged by AFM. Association was defined as any xylanase molecules on top of, or next to (i.e., within 5 nm of) the xanthan molecules. The total area of each scanned image was determined and the areas covered by either the xylanase or xanthan were measured. Using this information it was possible to determine the possibility of chance association, that is, these different molecules occupying the same area of mica. From these calculations it was confirmed that the small number of xylanase molecules found associated with the xanthan molecules could be explained purely by chance. No accumulation of xylanase molecules induced by the incubation process or the methods of sample preparation or imaging was detected. Hence the sampling process did not give rise to artifactual nonspecific binding. Similarly, in the polygalacturonase–arabinoxylan system, for all the polygalacturonase molecules analysed, only 0.001% were observed to be associated with arabinoxylan molecules, that is, either on or next to (within 5 nm of) arabinoxylan polymers. Again from this analysis it appears that the preparation stages do not introduce artifactual nonspecific binding of enzymes to the polysaccharides. Hence it can be concluded that the probability of observing nonspecific binding between arabinoxylans and xylanases is very low.

AFM images of the Xyn10A mutant E246A–arabinoxylan polymers are shown in Figure 2. The present studies are designed to test the feasibility of imaging inactivated enzymes bound to arabinoxylan chains and to develop methods for analysing such binding. For these studies it was considered sufficient to use molar ratios of enzyme to polysaccharide that would saturate the binding sites. The enzymes appear as round blobs (P) attached to the extended polymer chains. The measured heights of the blobs are consistent with the heights measured for AFM images of the individual enzymes. Figure 3 shows a plot of calculated protein volume against known molecular mass for proteins used in this study. The data show that the volume or height when compared with the values measured for the isolated proteins can be used to confirm the identity of the object bound to the polysaccharide. The majority of the mutant Xyn10A E246A molecules are seen attached to the arabinoxylan chains and very few unattached enzymes are seen in the images. The unattached enzymes seen in Figure 2a may have been knocked off the chains by the AFM probe. Imaging of the Xyn10A mutant E246A binding was difficult due to the small, but detectable, level of enzyme activity for this mutant: the length of the chains observed in the images varied with the preparation conditions. The images indicate that the binding is neither regular nor periodic and a range of different sized gaps was found between enzymes along the arabinoxylan polymers.

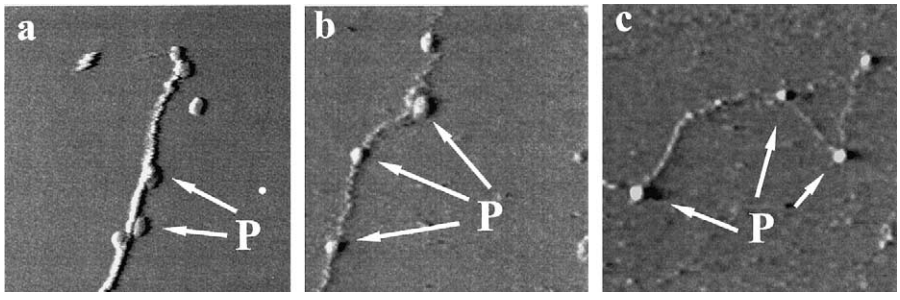

Figure 2. AFM images showing the binding of mutant Xyn10A xylanases (E246A) to arabinoxylan chains. Scan size 600×600 nm. The enzymes (P) are shown attached to the polysaccharide chains. In (a) there are two enzymes that have become detached from the chain. The enzymes are higher than the polysaccharide chains and it is possible that the probe has knocked the enzymes off the chain during scanning.

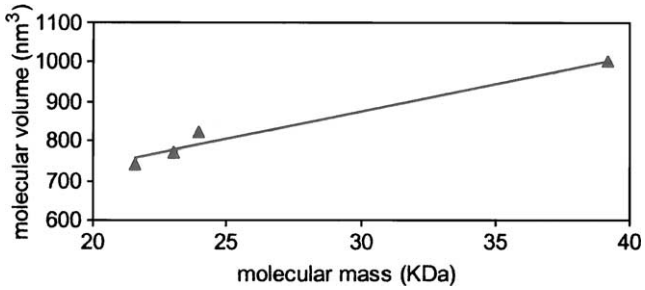

Figure 3. Graph showing the calculated volume of proteins imaged by AFM plotted against the molecular mass. The proteins used are a xylanase from *T. longibraciatum* (21.6 kDa), a xylanase from *N. patriciarium* (23 kDa), a polygalacturonase from *A. niger* (24 kDa) and a xylanase from *C. japonicus* (39.2 kDa).

The mutant Xyn11A E386A was derived from a family GH11 enzyme, and the mutant Xyn10A E246A was prepared from a family GH10 enzyme. Despite the fact that members of the families 10 and 11 catalyse the same reaction there are significant differences between the two groups. Family 10 xylanases can attack xylosidic linkages next to arabinose side chains and towards the nonreducing end, and require two unsubstituted xylose residues between side chains, whereas family 11 xylanases need three unsubstituted xylose residues between side chains.[25] Therefore, since the binding of family 10 xylanases to arabinoxylans is less affected by the presence of side chains than the binding of family 11 xylanases, the pattern of binding events would be expected to be different for the two mutant enzymes. The AFM images (Fig. 4) obtained do, indeed, appear to reveal different binding of mutant Xyn11A E386A xylanase along the arabinoxylan polymers when compared with that observed for the mutant Xyn10A E246A xylanase. A range of different binding patterns was detected, from areas that were unoccupied by xylanase molecules (arrow A, Fig. 4a), to blocks of xylanase molecules (arrow B, Fig. 4b). On initial visual examination of the images there does appear to be differences between the binding patterns of the two enzymes. There appears to be more clustering of the bound mutant Xyn11A E386A.

Pronounced clustering of the bound enzymes may be characteristic of a nonrandom binding pattern. However, it is difficult to draw this type of conclusion from just visual inspection of images. Thus some form of statistical analysis of images is important, in order to determine if the binding sites for both types of xylanases are randomly distributed along the arabinoxylan molecules. The control experiments indicated that, in the AFM images where xylanase molecules are seen to be associated with arabinoxylan molecules, this represents specific binding of the enzyme to the polysaccharide. Figure 5 shows a plot of the frequency of occurrence of pairs of bound mutant Xyn11A E386A xylanase enzymes as a function of their nearest neighbour separation distance along the chain. The expected distribution of binding sites on the chain will depend on the mechanism by which the chain is produced. If it is assumed that the creation of binding sites is a Poisson process in which active binding sites are formed at a constant density (λ) and the creation of new sites is independent of the formation of previous binding sites then the probability $P(x)$ of finding pairs of sites separated by a distance x will be $P(x) = \lambda \exp(-\lambda x)$. If the enzyme binding monitors the distribution of binding sites then the above equation should describe the data in Figure 5. It is important to try to test whether the binding sites are randomly distributed along the chains. This is because there are suggestions that arabinosylation may be denser on some parts of the chains than on others,[5,26] which may indicate some association between biosynthetic events that could influence binding of the

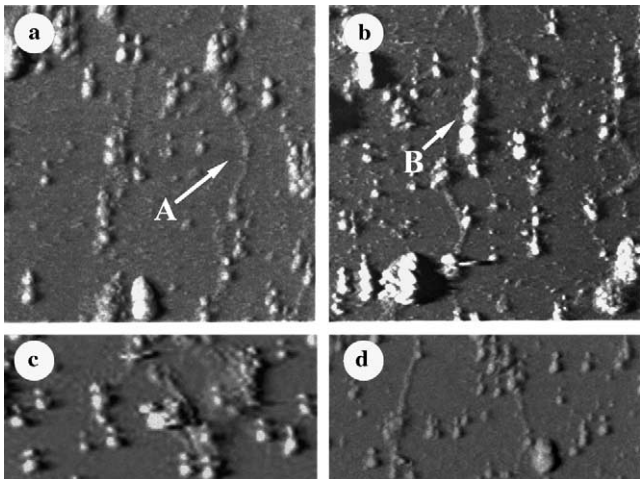

Figure 4. AFM images showing the binding of mutant Xyn11A xylanases (E386A) to arabinoxylan chains. Image size 600 × 600 nm. A indicates a region of the polysaccharide chain devoid of bound enzymes, B shows a cluster of bound enzymes.

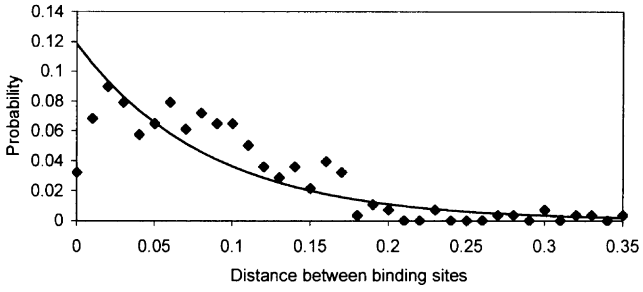

Figure 5. Graph showing the probability density function of bound enzymes with a given neighbour–neighbour separation (x) and a fitted exponential function $P(x)$.

probes. As can be seen the exponential function fits the experimental data at large separations, but fails at low separations. The data presented in Table 2 show a χ^2 analysis of the fit of the data to an exponential function. Examination of χ^2 tables confirms that the significance of a simple exponential function describing the experimental data is only 1 part in 1000. This is because the enzymes have a finite size and hence can only probe the distribution of binding sites over separations above the size of the enzyme. A bound enzyme carries an exclusion zone that prohibits visualisation of certain neighbouring binding sites. In effect the experiment will produce a probability distribution $P'(x) = g(x)\lambda\exp(-\lambda x)$, where $g(x)$ is a masking function that depends on the shape and size of the probe enzyme. The probability function $P'(x)$ can be approximated by a gamma distribution of the form $P'(x) = \lambda(\Gamma(\alpha))^{-1}(\lambda x)^{\alpha-1}\exp(-\lambda x)$. This is the simplest exponential function that contains sufficient parameters to model the cut-off at low enzyme separations. Figure 6 and Table 2 confirm that this type of distribution describes the experimental data very well. The data in Figure 6 demonstrate that, provided the gamma distribution is an adequate approximation for the masking effect, the distribution of binding sites on the polymer chain is random. This would suggest that there is no significance to the bare patch of chain or cluster of enzymes identified in Figure 4. It emphasises the need to analyse a large number of images rather than focus on images showing features that, due to their unusual form and visual impact, may attract undue attention. The high significance found for the fit of the experimental data to a gamma distribution (Table 2) suggests that this function may be the correct analytical solution for $P'(x)$. It should be possible to calculate the analytical form of $P'(x)$ since, in effect, it is the probability of finding segments of length δ distributed along the chain. The analysis of this problem is discussed further in the Appendix.

A similar analysis of the binding data for the mutant Xyn10A E246A is summarised in Table 2. The significance of the fit to a gamma distribution is reduced. A detailed analysis of this system is more difficult because

Table 2. χ^2 analysis of the selective binding data from AFM

	Mutant Xyn11A E386A	Mutant Xyn10A E246A	Mutant Xyn11A E386A+3 h
Exponential			
χ^2	224	171	346
Significance	0.001	0.001	0.01
Gamma			
χ^2	19	35	12
Significance	0.98	0.60	0.50

The significance is determined by the χ^2 value, the number of data points and χ^2 tables.

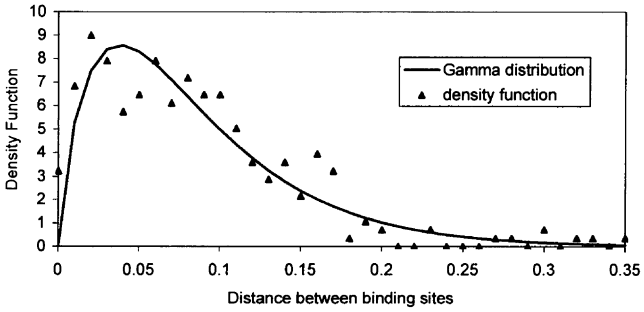

Figure 6. Graph showing the probability density function of bound enzymes with a given neighbour–neighbour separation (x) and a fitted gamma distribution function $P'(x)$.

of the small residual activity of this mutant enzyme. It is possible that the underlying binding site distribution is random and that the deviations are due to the low level of catalytic activity of the enzyme. The analysis presented in the appendix assumes that the population of chains can be approximated by an infinite length chain. The existence of finite length chains will cause a small departure from the expected gamma function. Additional cleavage of certain binding sites will increase the number of chain ends and will alter the observed distribution function of nearest-neighbour binding of the probes. This may be sufficient to reduce the fit to the gamma distribution. Further studies are required to test this suggestion.

If the arabinoxylan is treated with an arabinofuranosidase then this will reduce the number of arabinose side chains and should increase the number of xylanase binding sites. This effect should be significant for family 11 xylanases, which require three unsubstituted xylose residues next to an arabinose side chain.[25] If these new sites are created at a constant rate then the total number of binding sites per chain will increase but the distribution of binding sites as a function of their separation will remain the same. If, for example, the enzyme is bound to a site on the chain and then created a series of adjacent unsubstituted residues then the rate of creation of binding sites would not be constant, and both the number and the distribution of binding sites would change. It should be possible to investigate the action of arabinofuranosidase by examining the binding of inactive xylanases to the modified arabinoxylan molecules. Treatment of the arabinoxylan with the arabinofuranosidase for periods of 30 min, 1, 2 and 3 h led to progressive removal of side chains. At 3 h 10% of the arabinose had been removed. This was considered sufficient for the observation of the changes in the binding of the inactivated xylanase, but not too much to cause aggregation of the polysaccharides. Figure 7a–d shows the binding of the mutant Xyn11A E386A to an arabinoxylan that has been previously incubated with an arabinofuranosidase for 3 h. The images clearly demonstrate the expected increase of density of binding of

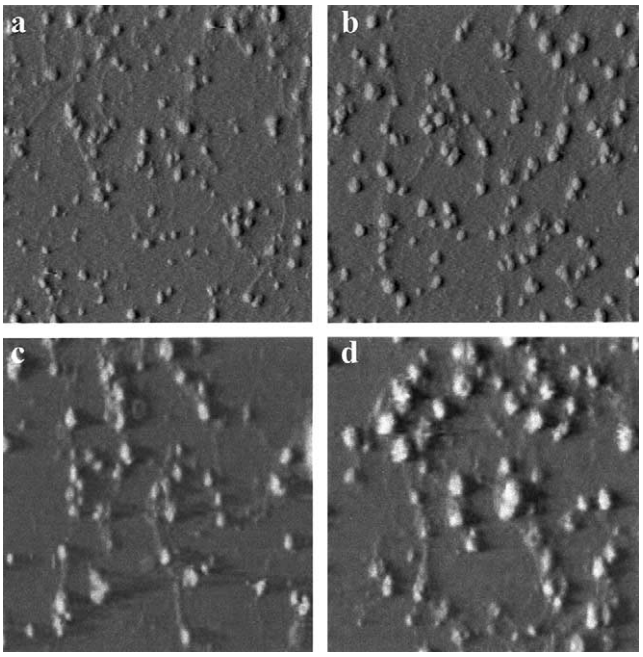

Figure 7. AFM images showing the binding of mutant Xyn11A xylanases (E386A) to arabinoxylan chains that have been treated with an arabinofuranosidase for 3 h. Scan size 600×600 nm.

the enzyme probes. Visually the images suggest that there does appear to be more evidence for clustering of these enzymes in the samples pre-treated with arabinofuranosidase for 3 h. To test whether this corresponds to preferential localisation of binding sites it is necessary to statistically analyse the images. Analysis of the data implies that the fit to a gamma distribution is less significant than for the untreated arabinoxylan (Table 2). This suggests that this approach can detect differences in the distribution of binding sites on the polysaccharide chains. Further analysis would require calculations of the expected distribution function $P'(x)$ based on models for the action of the arabinofuranosidase.

The present studies demonstrate that inactivated enzymes can be observed bound to arabinoxylan chains. This suggests that these mutant enzymes can be used to map and investigate the primary structure of heterogeneous polysaccharides. Preliminary analysis of the binding of inactivated family GH11 E386A xylanase suggest that the binding sites are distributed at random along the polysaccharide chains. Treatment of arabinoxylans with arabinofuranosidases was found to alter the binding of this inactivated xylanase to the polysaccharide chains. The present investigation demonstrates the feasibility of this approach. Clearly a considerable amount of further work would be needed to develop this approach as a routine tool for analysing modes of action of enzymes. The calculation of the expected nearest neighbour distribution functions for different modes of action of enzymes is not a trivial task. In the present experiments we have employed inactivated enzymes as structural probes. The same approach could be used to map the binding of other molecular probes to the polysaccharide chains. Examples of other probes might include lectins, antibodies or, preferably, FAB fragments or peptides generated by phage display technology with known epitopes. The experiments described above suggest a quantitative approach for analysing binding data. A simpler qualitative approach would be to use the probes to identify sub-populations of molecules with different structural features. There is clearly also potential for using such probes for mapping the location of particular polysaccharides within sectioned plant tissue. The use of enzymes, although not inactivated enzymes, as structural probes was pioneered by Seibert et al.[27] These authors used a fluorochrome–cellulase complex as a probe for cellulose in plant material. Later studies have employed a variety of probes including carbohydrate-binding domains, lectins and both polyclonal and monoclonal antibodies. Microbial enzymes from spoilage microorganisms have been evolved to degrade the native structural elements of plant tissue and use of inactivated clones of these enzymes provides a new source of molecular probes.

3. Experimental methods

3.1. Preparation of enzymes

3.1.1. Modification. Modified xylanases from both xylanase families (GH10 and GH11) were produced in order to determine the binding distributions of these enzymes on wheat flour arabinoxylan. Genetically modified xylanases were generated using site-directed mutagenesis. The catalytic nucleophile mutant Xyn10A E246A of xylanase from *C. japonicus*, wild-type Xyn10A, and Xyn11A mutants E386A (catalytic nucleophilic mutant) and E223S (catalytic acid/base mutant) from *N. patriciarium* were produced using the methodology described by Gilbert and co-workers.[28–30] N-Terminus protein sequencing of five terminal amino acids (carried out at the Protein Sequencing and Peptide Synthesis Facility at John Innes Centre, Norwich, UK) was used to confirm that the recombinant *N. patriciarium* xylanase had been purified from the *Escherichia coli* cells.

3.1.2. Purification of enzymes. Xylanase Xyn10A from *C. japonicus* was purified by FPLC (Amersham Pharmacia Biotech) using anion-exchange chromatography (MonoQ, HR 10/10, Amersham Pharmacia Biotech). Arabinofuranosidase from *A. niger* was purified by hydrophobic interaction chromatography (HIC; HiLoad 26/10 phenyl sepharose; Amersham Pharmacia Biotech). One of the controls used to check that any binding of enzymes observed by AFM was specific was

to investigate mixtures of arabinoxylans with enzymes known to have no activity towards arabinoxylans. The enzyme chosen for these studies was a polygalacturonase from *A. niger* (Megazyme) that was purified using anion-exchange chromatography.

3.1.3. Characterisation of enzymes. Xylanase activity was measured in the following manner. Arabinoxylan samples (2 mg mL^{-1}) were prepared in 2 mM ammonium bicarbonate buffer and incubated with the xylanase Xyn10A (10 μg mL^{-1}, *C. japonicus*) for 15 min at 30 °C. The reaction was stopped by the addition of dinitrosalicylic acid (DNS) reagent and the colour developed by boiling for 5 min. The absorbance was measured at 550 nm and the increase in reducing sugars was quantified using xylose or arabinose calibration curves (0–180 μg mL^{-1}). Arabinofuranosidase (*A. niger*; Megazyme Inc.) activity was determined in reaction mixtures of 0.5 mL containing 10 mM *p*-nitrophenyl-α-L-arabinofuranoside (pNPA) in 50 mM sodium acetate buffer, pH 4.0, incubated at 40 °C for 10 min. The reaction was terminated by the addition of 0.5 mL of 100 mM sodium tetraborate buffer. Release of free dye was measured spectrophotometrically at 400 nm. One unit of arabinofuranosidase activity was defined as the amount of enzyme releasing 1 μmol of sugar per minute at pH 4.0 at 40 °C. For the isoelectric focussing (IEF) determination of enzyme pI_a PhastGel isoelectric gel was run in accordance with the optimised method for an IEF 3–9 gel given in the manufacturer's technique file no 100.

3.1.4. Binding assay. To determine the percentage of bound enzymes over a given pH range a spectrofluorimetry method was developed. The substrate (water-insoluble wheat arabinoxylans WIAX, Megazyme) was used at a concentration of 25 mg mL^{-1} with an enzyme protein concentration at 1 mg g^{-1} of substrate, chosen so that the substrate would not be saturated by enzyme. The substrate was first equilibrated at the appropriate pH by washing with buffer until the pH of the buffer was unaltered by WIAX: WIAX has an initial buffering effect, and altered the pH of the buffer. In order to overcome this problem the WIAX samples were washed in the appropriate buffer until the pH remained constant and the buffer was then changed approximately three times following centrifugation (13,000g, 10 min, room temperature). The enzyme–substrate mixture was shaken for 30 min at 4 °C (to minimise hydrolysis), after which the sample was centrifuged and the supernatant was assayed for residual protein concentration by spectrofluorimetry (emission 350 nm, bandwidth 3 nm; excitation 280 nm, bandwidth 20 nm) and also using a dye-linked assay technique (Coomassie reagent). The buffers used were sodium-phosphate–sodium-citrate (McIlvaines buffer) at pH 3, 5 and 7 and Tris–HCl at pH 9. Bovine serum albumin was used as the standard protein to quantify residual protein in solution. Experiments were performed in triplicate. In order to assure that these assays probed specific binding of the enzymes two control experiments were devised. These involved xylanases and xanthan, a polysaccharide that does not specifically bind the enzyme, and arabinoxylans and polygalacturonase, an enzyme that does not specifically bind to the polysaccharide. To determine the level of any nonspecific binding between xylanase and xanthan, a 2 μL drop of xylanase (5 μg mL^{-1}) was deposited onto freshly cleaved mica sheets followed by a 2 μL drop of xanthan (2 μg mL^{-1}). Samples were allowed to dry at room temperature for 10 min and imaged by AFM under butanol using contact mode, using methods to be described later. This approach was also used for the imaging of arabino-xylans and polygalacturonase mixtures. The positive control, an active Xyn10A (*C. japonicus*) xylanase, was used to confirm that binding and subsequent hydrolytic activity was still present under AFM compatible conditions, that is, binding events occurred as a result of specific enzymic interaction, and not nonspecific absorption to the mica. Mixtures of active xylanase (5 μg mL^{-1}) and arabinoxylan (2 μg mL^{-1}) were prepared as described above for the negative control samples.

3.2. Preparation and characterisation of arabinoxylan samples

The isolation and characterisation of the water-soluble wheat arabinoxylans used in this study has been described in a previous publication.[23] The polymer was stored as a freeze-dried powder. For atomic force microscopy the samples were dissolved in 2 mM ammonium bicarbonate buffer at a concentration of 2 mg mL^{-1}. Protein was removed by overnight incubation with an immobilised protease.[23] Neutral sugars and glycosidic linkages were determined by methods described in detail elsewhere.[23] The ferulic acid and di-ferulic acid contents of the arabinoxylans were estimated by HPLC[31] following saponification with NaOH (1 M, 16 h, room temperature and pressure). The total protein content was determined by a Coomassie dye-binding assay[32] using bovine serum albumin (Sigma Aldrich) as a standard.

3.3. Size-exclusion chromatography (SEC)

Untreated and protease treated arabinoxylan samples were dissolved in a 2 mM ammonium bicarbonate buffer at a concentration of 2 mg mL^{-1}. This particular buffer concentration was found to be optimum for subsequent atomic force microscopy measurements. Samples (100 μL) were loaded onto a Polysep GFC P5000 column (Phenomenex, Macclesfield, Cheshire, UK), eluted at 0.5 mL min^{-1}, and the eluant monitored using a HP-

1047A refractive index detector (Hewlett Packard, Bristol, UK). Fractions were collected at 1 min intervals. Pullulan samples of molecular masses 166×10^4, 38×10^4, 18.6×10^4, 10×10^4, 4.8×10^4, 2.37×10^4, 1.22×10^4 and 0.58×10^4 were used as reference standards.

3.4. Atomic force microscopy (AFM)

3.4.1. Imaging of arabinoxylans. Fractions from the SEC column were concentrated by rotary evaporation to approximately $5\,\mu g\,mL^{-1}$. Samples (2 μL) were drop deposited onto freshly cleaved mica sheets. Typically samples were allowed to stand in air for about 10 min. The mica substrates were then placed in the liquid cell of the AFM and imaged under redistilled butanol. Butanol was used to reduce capillary forces (adhesion between the tip and sample) and hence to permit imaging at controlled, optimised applied forces, without damage or distortion of the sample. Images were obtained using an East Coast Scientific AFM working in the dc contact mode. The apparatus was calibrated using etched silicon Ultrasharp calibration gratings from NTMDT, Zelenograd Research Institute of Physical Problems, Moscow, Russia. The grating TGX01 was used for XY calibration and the gratings TGZ01-3 used for height calibration using step sizes of 25.5, 106 and 512 nm, respectively. Silicon nitride cantilevers were used with a quoted force constant of $0.38\,N\,m^{-1}$. Both topographic and error signal mode images were recorded. The AFM images are plane-fitted and renormalised by the ECS software. Image contrast was further optimised using Adobe Photoshop software.

3.4.2. AFM imaging of mutant xylanases and water-soluble arabinoxylan mixtures. In order to observe binding of xylanases to arabinoxylans AFM methods were developed to allow the repeatable imaging of these events. To observe binding for *C. japonicus* mutant xylanase, a 2 μL drop of the mutant Xyn10A E246A xylanase ($5\,\mu g\,mL^{1}$) was first deposited onto freshly cleaved mica and then allowed to stand in air for 10 min. The arabinoxylan samples (2 μL at $2\,\mu g\,mL^{-1}$) were deposited onto the same mica and allowed to stand in air for a further 10 min. This procedure was devised in order to reduce the time that the enzyme was in solution with the arabinoxylan as this enzyme was found to possess some degree of remaining activity. To observe the binding of the *N. patriciarium* mutant xylanases, a 2 μL drop of the xylanase ($5\,\mu g\,mL^{1}$) was deposited onto freshly cleaved mica. Then a 2 μL drop of the arabinoxylan sample ($2\,\mu g\,mL^{-1}$) was deposited before the sample had dried. The mica was kept wet for a 10 min incubation period by the addition of 2 mM ammonium bicarbonate buffer. This was to allow time for the enzyme to interact with the substrate and for binding to occur. The sample was allowed to stand in air for 10 min.

3.4.3. AFM imaging controls. Methods for imaging the xylanase binding to arabinoxylans were developed in order to be able to image consistently these events. A number of control experiments were developed in order to demonstrate the effectiveness of the technique for observing the specific binding of xylanases and arabinoxylan. In order to eliminate possible artifacts due to the substrate and the buffer solutions used ammonium bicarbonate (2 mM) was deposited onto mica and allowed to dry for 10 min at room temperature. Samples were then imaged under butanol by AFM. This was to investigate the surface structure of the mica and the purity of the buffer used. Sublimation of the buffer did not generate any unwanted artifacts on the mica substrate. The xylanase–arabinoxylan mixtures and the control mixtures of xylanase–xanthan and polygalacturonase–arabinoxylan were prepared and scanned using identical experimental conditions.

3.5. Enzymatic treatment of arabinoxylan samples

3.5.1. Xylanase treatment. An arabinoxylan sample, collected at 13 min from the SEC fractionation column, was incubated with *C. japonicus* xylanase ($25\,\mu g\,mL^{-1}$) at 30 °C for periods of 5 or 10 min. The reaction was stopped by either depositing 2 μL of the sample onto mica (for AFM analysis), by adding DNS reagent (for reducing sugar analysis), or by boiling for 5 min (SEC analysis).

3.5.2. Arabinofuranosidase treatment. Arabinoxylan samples (100 μg, prepared in 2 mM ammonium bicarbonate) were incubated with arabinofuranosidase (37 °C, pH 6.0) in a final volume of 1.2 mL for time periods of 0.5, 1, 2 and 3 h. To further confirm that the arabinofuranosidase activity was free of contaminating xylanase activity, TMS modification of sugars was applied. These samples were spun through a concentrating device (10 min, 13,000g, room temperature) with a molecular cut-off at 3000 (Viva Science) to separate polymers and proteins from released oligomers and sugars. Bis-trimethylsilylimidazole (BSTFA; 100 μL) was added to each sample, prior to heating (30 min, 70 °C). Samples were allowed to cool to room temperature and then analysed by GC/MS. GC/MS analysis was performed with a Hewlett Packard HP-5890 coupled to a Tris-1S mass spectrometer (Micromass, UK) operated in EI mode. A DB-1 fused-silica capillary ($30\,m\times0.32\,\mu m$ film thickness, J&W Scientific) was operated at a helium carrier gas flow rate of $1\,mL\,min^{-1}$. The samples were injected at a temperature of 250 °C into the split injector 40:1. The GC was temperature programmed to run from 120 to 180 °C at $1\,°C\,min^{-1}$

and then 180 to 230 °C at 2 °C min^{-1}. EI mass spectra were obtained in the range m/z 50–800 every 1.0 s using a source temperature of 200 °C and an ionisation voltage of 70 eV. The quantification of the amount of arabinose released was determined from the peak area at 20.80 min, following the comparison of this peak fragments with an MS library of sugar fragments produced following TMS modification of the sugars.

3.6. Analytical methods of AFM images

To determine the distribution of enzyme binding along the arabinoxylan molecules analytical methods were developed. These methods were applied to both test and control samples imaged by AFM.

3.6.1. Analysis of arabinoxylan polymers imaged by AFM. The images were assessed using Image tool (Uthscsa). Measurements were taken of the distances between binding events along the arabinoxylan chains. The molecular size (heights) of the molecules bound to the chains was used to confirm the identity of the bound protein molecules.

3.6.2. Analysis of isolated enzymes by AFM. This analysis was developed from methods proposed by Schneider et al.[33] in order to confirm that the molecules found to be bound to the arabinoxylan were indeed the proteins of interest. Enzymes were imaged alone at a concentration that produced an even coverage of discrete enzyme molecules on the mica (approximately 5 μg mL^{-1}). Multiple cross-sections of the individual proteins were measured to establish the mean diameters and heights of each single protein. During scanning the tip will partially compress the enzymes reducing the expected height values and altering the shape of the enzymes. In addition the measured radii will be broadened by an amount that depends on the geometry of the scanning tips. If the scanning tip can be approximated by a hemisphere of radius R then, if the maximum measured broadened radius of the molecules is w, the true molecular radius will be $r = w^2/16R$. The Schneider et al.'s approach[33] suggests calculating the molar volume by approximating the enzymes as segments of a sphere of volume $V = (h/6)(3r^2 + h^2)$. These calculated volumes are plotted as a function of the known molecular masses of the xylanases used in the present study in Figure 3. The volume and hence the measured height of the proteins was found to increase with increasing molecular mass. Although this approach is approximate it was found that height or volume measurements were sufficient to identify molecules bound to arabinoxylans, based on the dimensions of the isolated proteins when imaged on mica.

Appendix. Irreversible adsorption on a disordered 1D lattice

For a Poisson process a set of active binding sites will be distributed along an infinite line with constant density λ.

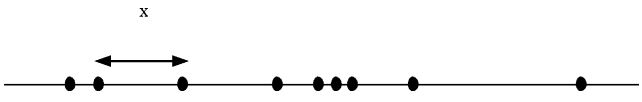

The nearest neighbour site separations will have an exponential distribution:

$$P(x) = \mathrm{Exp}(\lambda) = \lambda \mathrm{e}^{-\lambda x} \equiv Gamma(1, \beta) \qquad (1)$$

where $\beta = \lambda^{-1}$ and *Gamma* represents a Gamma distribution

$$Gamma(\alpha, \beta) = \beta^{-\alpha} x^{\alpha-1} \mathrm{e}^{-x/\beta} / \Gamma(\alpha) \qquad (2)$$

In the case of irreversible, saturated, adsorption at the active sites the adsorption positions will reveal the exponential distribution of nearest neighbour site separations.

However, the exponential distribution includes a finite weight at infinitesimal site separations. Therefore this model will include some un-physical adsorbed configurations.

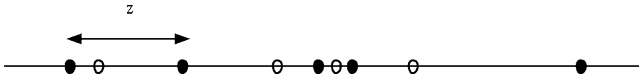

For sequential progression along the line, with adsorption only occurring at non-adjacent sites (this approximation neglects configurations, which arise in random adsorption processes, where two unoccupied sites are trapped between two occupied sites), the spatial distribution of the adsorbed species will follow the distribution of the doublet lengths of the lattice:

$$\begin{aligned} P(z = x_1 + x_2) &= \int_0^\infty \int_0^\infty \lambda \mathrm{e}^{-\lambda x_1} \lambda \mathrm{e}^{-\lambda x_2} \delta(z - x_1 - x_2)\, \mathrm{d}x_1\, \mathrm{d}x_2 \\ &= Gamma(2, \beta) \end{aligned} \qquad (3)$$

Since $Gamma(\alpha_1, \beta) + Gamma(\alpha_2, \beta) = Gamma(\alpha_1 + \alpha_2, \beta)$ this result may be generalised so that a series of gamma distributions, $Gamma(3, \beta)$, $Gamma(4, \beta)$ etc., describe triplet, quadrouplet etc. lengths on the lattice.

However, in turn, this approximation allows an adsorption event to shield a neighbouring site from future events, even when the sites are well separated. More accurately, one may consider an inactivated region, of

size δ, surrounding each adsorption site. In this case the distribution of separations for the adsorbed species will be a combination of singlet, doublet, triplet etc. separations. Thus, again working sequentially along the line,

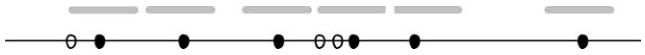

$$\begin{aligned} &P(\text{separation of adsorption events} = x > \delta) \\ &\quad = P(\text{singlet separation} = x) + P(\text{doublet separation} \\ &\quad = x \cap \text{singlet separation} < \delta) + P(\text{triplet separation} \\ &\quad = x \cap \text{doublet separation} < \delta) + \ldots \end{aligned}$$

The terms on the right hand side of this expression can be written as integrals:

$$\begin{aligned} &P(n-\text{tuplet separation} \\ &\quad = x \cap (n-1) - \text{tuplet separation} < \delta) \\ &\quad = \int_0^{\delta} P(\text{singlet separation} = x - \varepsilon \cap (n-1) \\ &\qquad - \text{tuplet separation} = \varepsilon)\,\mathrm{d}\varepsilon \\ &\quad = \int_0^{\delta} \frac{\beta^{-1}\mathrm{e}^{-(x-\varepsilon)/\beta}}{\Gamma(1)} \frac{\beta^{-(n-1)}\varepsilon^{n-2}\mathrm{e}^{-x/\beta}}{\Gamma(n-1)}\mathrm{d}\varepsilon \\ &\quad = \frac{(\delta/\beta)^{n-1}}{\Gamma(n)} Gamma(1,\beta) \quad n > 1 \end{aligned}$$

where the independence of individual lattice separations and the Gamma distribution representation for n-tuplet distances has been used. It is straight forward to sum these terms so that the probability distribution for separations of a given δ, $P'(x|\delta)$, will be a shifted exponential distribution:

$$P'(x|\delta) = \mathrm{e}^{\delta/\beta} Gamma(1,\beta) \quad x > \delta$$

Without details of the prior distribution, $P(\delta)$, of the inactivation lengths it is not possible to establish the full marginal (observed) distribution of adsorption separations, $P'(x)$. From the above equation it is clear that, at large separations, $P'(x)$ will decay as $\mathrm{e}^{-x/\beta}$. If, additionally, one assumes that δ has a narrow distribution centred on its mean value, $\langle\delta\rangle$, it is reasonable to assume that $P'(x)$ can be approximated by a single Gamma distribution, with scale β, that is equi-modal with $P'(x|\langle\delta\rangle)$:

$$P'(x) \sim Gamma(1 + \langle\delta\rangle/\beta, \beta)$$

Random sequential adsorption, i.e. not arranged sequentially along the line, will lead to configurations that are more complex than those described above.

Acknowledgements

This research was supported by the BBSRC core strategic grant to IFR and by a BBSRC studentship awarded to E. L. Adams. At IFR the authors wish to thank Steve Ring and Kate Kemsley for discussions and Andrew Kirby and Patrick Gunning for help with the AFM measurements. At Newcastle the authors thank Carl Morland for purifying the enzymes used in this study. The analysis presented in the Appendix was suggested and developed by Gary Barker at IFR.

References

1. Lempereur, I.; Rouau, X.; Abecassis, J. *J. Cereal Sci.* **1997**, *25*, 103–110.
2. Bengtsson, S.; Aman, P.; Andersson, R. *Carbohydr. Polym.* **1992**, *17*, 277–284.
3. Ahluwalia, B.; Fry, S. C. *J. Cereal Sci.* **1986**, *4*, 287–295.
4. Izydorczyk, M. S.; Biliaderis, C. G. *Cereal Chem.* **1993**, *70*, 641–646.
5. Izydorczyk, M. S.; Biliaderis, C. G. *Carbohydr. Polym.* **1995**, *28*, 33–48.
6. Chanliaud, E.; Roger, P.; Saulnier, L. *Carbohydr. Polym.* **1996**, *31*, 41–46.
7. Dervilly, G.; Saulnier, L.; Roger, P.; Thibault, J.-F. *J. Agric. Food Chem.* **2000**, *48*, 270–278.
8. Chanliaud, E.; Saulnier, L.; Thibault, J.-F. *J. Cereal Sci.* **1995**, *21*, 195–203.
9. Delcour, J. A.; Vanhamel, S.; Hoseney, R. C. *Cereal Chem.* **1991**, *68*, 72–76.
10. Fincher, G. B.; Stone, B. A. In *Advances in Cereal Science and Technology*; Pomeranz, Y., Ed.; American Association of Cereal Chemists: St Paul, 1986; p 267.
11. Gruppen, H.; Kormelink, F. J. M.; Voragen, A. G. J. *J. Cereal Sci.* **1993**, *18*, 111–128.
12. Hoffmann, R. A.; Roza, M.; Maat, J.; Kamerling, J. P.; Vliegenthart, J. F. G. *Carbohydr. Polym.* **1991**, *15*, 415–430.
13. Izydorczyk, M. S.; Biliaderis, C. G. *Carbohydr. Polym.* **1994**, *24*, 61–71.
14. Beg, Q. K.; Kapoor, M.; Mahajan, L.; Hoondal, G. S. *Appl. Microbiol. Biotechnol.* **2001**, *56*, 326–338.
15. Kaneko, S.; Ishii, T.; Kobayashi, H.; Kusakabe, I. *Biosci. Biotechnol. Biochem.* **1998**, *62*, 695–699.
16. Derewenda, U.; Swenson, L.; Green, R.; Wei, Y. Y.; Morosoli, R.; Shareck, F.; Kluepfel, D.; Derewenda, Z. S. *J. Biol. Chem.* **1994**, *269*, 20811–20814.
17. Fushinobu, S.; Ito, K.; Konno, M.; Wakagi, T.; Matsuzawa, H. *Protein Eng.* **1998**, *11*, 1121–1128.
18. Lo Leggio, L.; Jenkins, J.; Harris, G. W.; Pickersgill, R. W. *Proteins—Struct. Func. Genet.* **2000**, *41*, 362–373.
19. Zechel, D. L.; Withers, S. G. *Acc. Chem. Res.* **2000**, *33*, 11–18.
20. Wakarchuk, W. W.; Campbell, R. L.; Sung, W. L.; Davoodi, J.; Yaguchi, M. *Protein Sci.* **1994**, *3*, 467–475.
21. White, A.; Withers, S. G.; Gilkes, N. R.; Rose, D. R. *Biochemistry* **1994**, *33*, 12546–12552.
22. Bennett, N. A.; Ryan, J.; Biely, P.; Vršanská, M.; Kremnicky, L.; Macris, B. J.; Kekos, D.; Christakopoulos, P.; Katapodis, P.; Claeyssens, M.; Nerinckx, W.; Ntauma, P.; Bhat, M. K. *Carbohydr. Res.* **1998**, *306*, 445–455.
23. Adams, L. A.; Kroon, P. A.; Williamson, G.; Morris, V. J. *Carbohydr. Res.* **2003**, *338*, 771–780.

24. Gunning, A. P.; Mackie, A. R.; Kirby, A. R.; Kroon, P.; Williamson, G.; Morris, V. J. *Macromolecules* **2000**, *33*, 5680–5685.
25. Biely, P.; Vršanská, M.; Tenkanen, M.; Kluepfel, D. *J. Biotechnol.* **1997**, *57*, 151–166.
26. Perlin, A. S. *Cereal Chem.* **1951**, *28*, 382–393.
27. Seibert, G. R.; Benjaminson, M. A.; Hoffman, H. *Stain Technol.* **1978**, *53*, 103–106.
28. Gilbert, H. J.; Sullivan, D. A.; Jenkins, G.; Kellett, L. E.; Minton, N. P.; Hall, J. *J. Gen. Microbiol.* **1988**, *134*, 3239–3247.
29. Gilbert, H. J.; Hazelwood, G. P.; Laurie, J. I.; Orpin, C. G.; Xue, G. P. *Mol. Microbiol.* **1992**, *6*, 2065–2072.
30. Hall, J.; Hazelwood, G. P.; Huskisson, N. S.; Durrant, A. J.; Gilbert, H. J. *Mol. Microbiol.* **1989**, *3*, 1211–1219.
31. Kroon, P. A.; Williamson, G. *J. Sci. Food Agric.* **1999**, *79*, 355–361.
32. Bradford, M. M. *Anal. Biochem.* **1976**, *72*, 248–254.
33. Schneider, S. W.; Larmer, J.; Henderson, R. M.; Oberleithner, H. *Pflugers Arch.—Eur. J. Physiol.* **1998**, *435*, 362–367.